

Article

# Fabrication and Characterization of Copper and Copper Alloys Reinforced with Graphene

Antoine Bident <sup>1,3</sup>, Nathalie Caillault <sup>3</sup>, Florence Delange <sup>3</sup>, Christine Labrugere <sup>4</sup>, Yongfeng Lu <sup>2</sup> and Jean-François Silvain <sup>1,2</sup>

<sup>1</sup> Univ. Bordeaux, CNRS, Bordeaux INP, ICMCB, UMR 5026, 33600 Pessac, France

<sup>2</sup> Department of Electrical and Computer Engineering, University of Nebraska-Lincoln, Lincoln, NE 68588-0511, USA

<sup>3</sup> Schneider Electric SAS, 38 EQI, Rue Henry Tarze, 38000 Grenoble, France

<sup>4</sup> CNRS, Univ. Bordeaux, PLACAMAT, UMS 3626, F-33608 Pessac, France

\* Correspondence: jean-francois.silvain@icmcb.cnrs.fr; Phone: +33 (0)540006437

**Abstract:** The constant increase in current density in electrical wires leads to increasingly significant heat losses due to Joule effect. Therefore, reducing the electrical resistivity of copper wires becomes necessary. To achieve this goal, the development of a composite material incorporating a more conductive reinforcement, the graphene, is a promising way. The design of a copper/graphene composite using a powder metallurgy-based method is presented. This synthesis method allows for interface control through the growth of CuO(Cu) nanoparticles tightly bonded to the reinforcement. It also involves the dispersion of graphene through ultrasonic treatment and its alignment within the matrix using a uniaxial pressing densification method. The increase in the hardness (+12 HV) demonstrates the effective dispersion and separation of graphene layers. The impact on the electrical properties of dendritic copper ( $\rho_e = 2.30 \mu\Omega\cdot\text{cm}$ ) remains limited, with a decrease in electrical resistance of approximately 1.4%. However, for copper with higher electrical resistivity, flake copper (at  $2.71 \mu\Omega\cdot\text{cm}$ ) and brass at ( $7.66 \mu\Omega\cdot\text{cm}$ ), reductions of 2.7% and 10% have been achieved, respectively. With the improvement of graphene quality, there is more room to improve the electrical properties. This work paves the way for the development of composites with improved electrical resistivity.

**Keywords:** graphene; surface treatment; hardness; electrical conductivity; composites; copper; powder methods

---

## 1. Introduction

Currently, copper (Cu) is the most widely used metal for electrical systems. This is mainly due to its mechanical properties, particularly its ductility which allows for easy shaping; as well as its electrical resistivity, which is among the lowest among metals ( $1.78 \mu\Omega\cdot\text{cm}$  at  $20^\circ\text{C}$  [1]). When a significant current density is applied to an electrical system, a non-negligible portion of energy is lost as heat. This phenomenon is known as Joule heating, and can result in energy losses (close to 10% according to l'IEA [2]) and potentially damage to the system if not properly managed. The use of a material with a lower electrical resistivity appears to be a viable solution to address this issue.

Only silver (Ag) can meet this criterion. However, but the expensive costs exclude itself from industrial applications ( $8,8 \text{ €/kg}$  for Cu against  $750 \text{ €/kg}$  for Ag [3]). An alternative is to develop a composite material using a reinforcement that is less resistive than Cu. From our knowledge, only graphene (Gr) can fulfil this requirement. Known since the 1960s, it was only in 2004 that K. Novoselov and A. Geim [4] were able, for the first time, to isolate graphene sheets using mechanical exfoliation, commonly called the "scotch trick". The great attraction of scientists to this 2D material comes from the  $\text{sp}^2$  hybridization of carbon atoms, which allows for the delocalization of the  $\text{P}_z$  orbital directed perpendicularly to the graphite plane. The overlapping of these  $\text{P}_z$  orbitals allows the formation of  $\pi-\pi^*$  bonds, which are responsible for amazing electronic properties [5,6]. As a result, Gr has a unique band structure with a semiconductor-like behaviour with a zero bandgap. These characteristics of Gr lead to exceptional electrical properties ( $200,000 \text{ cm}^2/\text{Vs}$  [7]), thermal

properties (5600 W/mK [8]), and mechanical properties (Young's modulus of 1 TPa and tensile strength of 130 GPa [9]). Due to these properties, the Gr has been used as a reinforcement in various types of composite materials such as polymers, metals, or ceramics. However, the different methods to fabricate these composites have their own advantages and disadvantages that affect the final properties. Nevertheless, based on powder metallurgy (used in this study), three main points are important to master in order to obtain a high-performance composite material.

The first two factors to be considered are the distribution [10] and orientation of the Gr reinforcement within the matrix [11]. An agglomeration of several graphene layers or a significant overall misorientation of the reinforcement will result in the degradation of the macroscopic properties of the composite materials. The reinforcement-matrix (R-M) interface is also critical for ensuring proper transfer of properties between both materials. However, Cu and carbon have no chemical affinities leading to a poor interfacial property transfer. Two methods exist to create interfacial chemical bonding : the first involves using a carbide element which will react with carbon to form carbide interphase [12]. However, the formation of this carbide interphase is associated with the reaction of carbon and therefore of the degradation and/or the total of consumption of Gr, making this method inappropriate for nanometric carbon-based reinforcement. The second method involves the growth of metallic nanoparticle, chemically linked with the carbon atom surface of Gr, on the surface of the reinforcement [13]. These particles can be made from various materials (Cu, Ag, Cr, Ni...[14,15]). Cu will be chosen to match the matrix. Nevertheless, there are very few articles reporting a decrease in electrical resistivity of such a composite compared to pure Cu. Keerti S. et al. [16] show a 2.7% increase in electrical conductivity of pure Cu with the incorporation of 15 ppm (0.006% vol.) of graphene, while Mu Cao's team [17] obtained over 15% increases in electrical conductivity compared to pure Cu. However, the fabrication method employed by the latter is too sophisticated to be viable for industrial applications. Nevertheless, some studies [18,19] have reported an increase in electrical resistivity on Cu.

In this work, Cu/Gr and brass/Gr composite materials were fabricated using conventional powder metallurgy processes. Specific surface treatment of Gr surface allows to add nanometric particles of Cu chemically linked with Gr. Hardness and electrical conductivity were measured on each sample and compared to non-reinforced materials.

## 2. Materials and Methods

### 2.1. Raw materials

Dendritic Cu (Cu-D) powder with an average length size of 50  $\mu\text{m}$  and a diameter of 10  $\mu\text{m}$ , and flake Cu (Cu-P) powder with an average width of 20  $\mu\text{m}$  and a thickness of 350 nm were purchased from ECKART. Flake brass (Bra-P) (80% Cu, 20% Zn) powder, purchased from Werth-Metal, has an average length size of 40  $\mu\text{m}$  and a diameter of 10  $\mu\text{m}$ . These powders were used as received without further treatment. Multilayer Gr powder (KNG-5) with a lateral size of 5-10  $\mu\text{m}$  and an average thickness of 2-3 nm (3-9 atomic layers) were bought from KNANO Company. This MLG was made by a chemical exfoliation method.

#### 2.1.1. Fabrication of the composite materials

First, homogenization of the Gr reinforcement in an ethanol solution of 0.1 g/L concentration was carried out using an acoustic mixer, with an acceleration of 80 g for 6 min. An acoustic type mixer (LABRAM II Resodyn) was then used in order to reach an optimal "matrix + reinforcement". In this process, the "ethanol + Gr solution" was spread on the surface of the Cu powders which were in levitation induced by the acoustic wave of the mixer. In order to reduce the surface oxidation of the Cu powder as well as the CuO nanoparticles, the composite powder "Cu + Gr" obtained was dried and reduced in a furnace at 400  $^{\circ}\text{C}$  for 60 min under a flow of Ar/5% H<sub>2</sub>. The densification of the composite materials was carried out using a Thermolab press equipped with an inductive heating system. The densification parameters are a temperature of 650  $^{\circ}\text{C}$  applied for 45 min under a pressure of 60 MPa in an inert atmosphere. Relative densities, equal or greater than 99% whatever the materials, were measured using the Archimedes' displacement method.

### 2.1.2. Characterization method

Hardness of different materials was measured using the Micro-Vickers hardness method, in the plane perpendicular to the densification direction, using a force of 20 kgf. The electrical resistivity of the composites was measured by typical a four-point contact probe. Both outer tips are connected to the generator for current injection with an ammeter for current measurement. Both inner tips are connected to a nano-voltmeter for voltage measurement. This system was placed in a temperature-controlled oven to perform measurements at various temperatures. A thermocouple was also placed under the sample to obtain an accurate temperature value.

Cu nanometric particles were characterized by transmission electron microscopy (TEM) using a JEOL-2100 microscope. Analysis of the Gr surface was carried out using a ThermoFischer Scientific K-Alpha® X-ray photoelectron spectrometer system with a monochromatized Al K $\alpha$  source ( $h\nu = 1486.6$  eV) and a spot size of 200  $\mu\text{m}$ . Full and high-resolution spectra obtained were fitted using the AVANTAGE software provided by ThermoFischer Scientific®. Scofield sensitivity factors were used for quantification. The measurements were conducted with a precision of 0.1  $\text{cm}^{-1}$  using a high-resolution Jobin Yvon Horiba LabRam HR micro-Raman spectrometer equipped with a charge coupled device (CCD) detector. Raman spectra were obtained in scattering micro-configuration. The incident laser light as well as the backscattered light are focused by a 10 $\times$  objective.

## 3. Results and Discussion

### 3.1. Determination of the optimal amount of Gr reinforcement

To determine the percolation threshold value for an "ideal" material, where half of the metallic powders are covered by one Gr sheet, the calculation of the required Gr content is proposed. The aim is to avoid the contact between two Gr particles during the assembly of the Cu powder, which would result in the presence of nano-porosity I between 2 Gr sheets which is assumed to be harmful for the electrical properties.

The geometry of the KNG-5 Gr and Cu-P powder are taken into account in these calculations. First, the **Equation 1** allows to calculate the surface areas of Cu and Gr particles.

$$S_{Cu} = \frac{(1-\%wt)}{V_{Cu} \times \rho_{Cu}}; \quad S_{Gr} = \frac{\%wt}{V_{Gr} \times \rho_{Gr}}, \quad (1)$$

where  $S_{Cu}$  and  $S_{Gr}$  are the surface areas of Cu and Gr in  $\text{cm}^2$ ,  $\%wt$  is the weight percentage of the reinforcement,  $\rho_{Cu}$  and  $\rho_{Gr}$  are the density of Cu (8.9  $\text{g}/\text{cm}^3$ ) and graphene (2.2  $\text{g}/\text{cm}^3$ ), respectively, and  $V_{Cu}$  and  $V_{Gr}$  are the volumes of Cu and graphene particles in  $\text{cm}^3$ .

To determine the coverage percentage of Cu by Gr particles, we need to calculate the ratio of the surface areas of the Gr particles to those of the Cu particles. This can be done using the following equation (2), with its representation in Figure 1.

$$\frac{S_{Gr}}{S_{Cu}} = \frac{\frac{\%wt}{V_{Gr} \times \rho_{Gr}}}{\frac{(1-\%wt)}{V_{Cu} \times \rho_{Cu}}} = \frac{\%wt \times V_{Cu} \times \rho_{Cu}}{(1-\%wt) \times V_{Gr} \times \rho_{Gr}}. \quad (2)$$

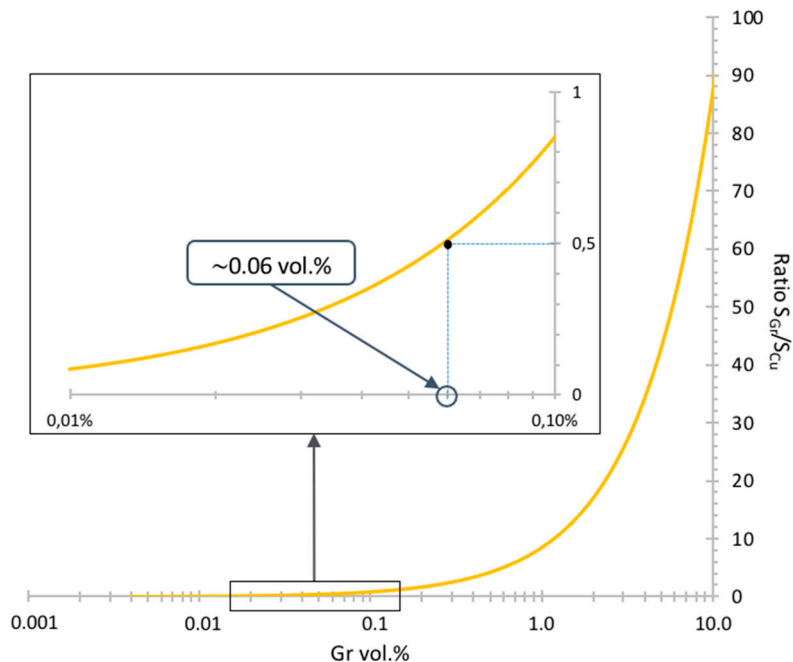


**Figure 1.** Evolution of the  $S_{Gr}/S_{Cu}$  ratio as a function of the percentage of Gr inside the composite materials.

According to this graph, a quantity of 0.06 vol.% of graphene seems sufficient to cover half of the surface areas of the Cu-P powders. In the case of our materials, a quantity of graphene corresponding to an initial content of 0.1 vol.% were used to compensate for losses induced by the various steps. The same Gr amount were for both dendritic Cu and Brass flakes.

The calculated Gr content may seem low compared to the majority of the recent works in the literature [20], where graphene contents higher than 1 vol.% were used. However, as seen in various works [21], percolation thresholds around 0.1 vol.% are often obtained.

As mentioned previously, Cu and Gr are two materials chemically inert. Therefore, a preparation step of the Gr reinforcement, including chemical treatment of Gr and germination-growth of nanometric Cu particles onto Gr surface, is necessary.

### 3.2. Surface treatment and functionalization of the graphene materials

To disperse the Gr materials, acoustic mixing (80 g for 10 min) has been applied on alcohol + Gr mixture. After this first treatment, nitric acid (HN) treatment has been used to modify the surface chemistry of the Gr powder. Specific conditions of the mixing and acid treatment can be found in [22]. Treatment time ranging from 0 to 150 min, at a temperature of 100 °C under magnetic stirring, has been performed. XPS analysis has been performed to characterize the evolution of the surface chemistry of the non-treated and treated Gr powders. Table 1 shows the evolution of the carbon (C1s) and oxygen (O1s) percentages with the treatment time. No specific effect can be observed. After deconvolution of the C1s spectra, Table 2 shows the evolution of the  $C_{sp^2}$  and  $- *$  percentage and the  $C_{sp^2}/C_{sp^3}$  ratio. In the two-dimensional structure of Gr, each carbon atom is strongly bonded to three neighbors ( $\sigma$  bonds) with an angle of 120° in the plane. This structure is the consequence of the  $sp^2$  hybridization of the carbon atoms and the  $sp^3$  hybridization is related to the disorder or amorphous carbon. This configuration allows the non-hybridization (delocalization) of the carbon p<sub>z</sub> orbital which is found directed perpendicular to the graphitic plane. It is the overlapping of these orbitals that allows the formation of the  $\pi-\pi^*$  bonds that are the origin of the astonishing electronic properties of Gr [23].

**Table 1.** Evolution of the O and C percentages: XPS analysis of the HN treated and non-treated Gr materials.

| Treatment time (min) | C (%) | O (%) |
|----------------------|-------|-------|
| 0                    | 98.5  | 1.5   |
| 30                   | 98.5  | 1.5   |
| 150                  | 98.5  | 1.5   |

Table 1 shows that the HN treatment has no effect on the evolution of the chemistry of the Gr surface (C and O are constant, independent of the treatment time). After deconvolution of the high-resolution C peak, Table 2 shows that the concentration of the  $C_{sp^2}$  species increases with the treatment time. It seems unlikely that this increase is attributable to a "restoration" of the graphitic network. It is more likely that the acid treatment leads to the elimination of surface contamination from the Gr materials.

**Table 2.** Evolution of the C1s contributions with different HN treatment time.

| Treatment time (min) | $C_{sp^2}$ (%) | $C_{sp^2}/C_{sp^3}$ | $\pi - \pi^*$ (%) |
|----------------------|----------------|---------------------|-------------------|
| 0                    | 69.0           | 10.3                | 9.3               |
| 30                   | 70.5           | 13.4                | 8.6               |
| 150                  | 73.0           | 15.1                | 7.6               |

However, with regard to the evolution of the percentage of the  $\pi - \pi^*$  bonds, the material seems to undergo a slight degradation (cf. Table 2). Therefore, a short treatment time is preferable to limit deterioration and eliminate some of the contamination. A time of 30 min was therefore selected.

To enable the germination growth of copper nanoparticles on the entire surface of the reinforcement, a dispersion step of the graphene in the solution (ethanol) is necessary. To achieve this, ultrasonic agitation for a time ranging from 10 sec to 90 min was performed. To monitor the evolution of the separation of the graphene layers, an analysis by UV-Visible spectroscopy was performed (cf. Figure 2). In our case, since the graphene serves as a density filter, an increase in the absorbance of the solution would indicate an increase in the amount of layers present, i.e., exfoliation of the graphene layers.

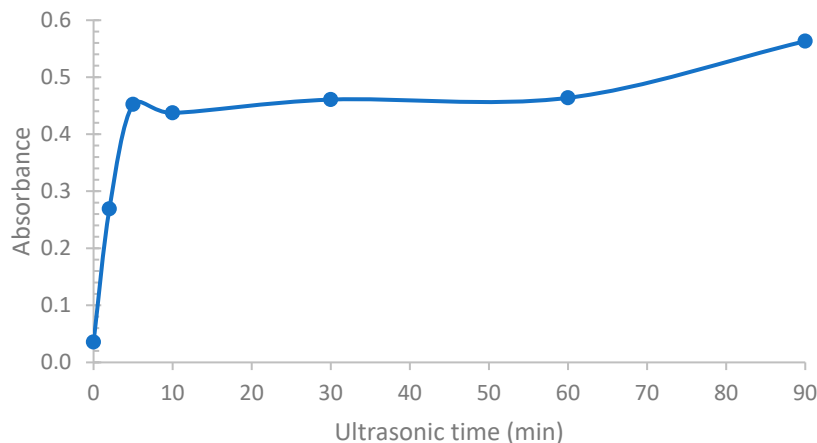


**Figure 2.** Evolution of the absorbance of different Gr solutions after various ultrasonic treatment times.

As can be seen, an increase in the ultrasonic treatment time leads to an increase in the absorbance of the solution. This graph also shows that the separation of the layers reaches its maximum after a 5 min treatment, with the absorbance of the solution remaining constant up to an hour of treatment. Raman analyses, allowing the calculation of the  $I_D/I_{2D}$  ratio (used instead of the  $I_D/I_G$  ratio for higher sensitivity), show that during this first hour, the reinforcement is not degraded by the ultrasonic treatment (Table 3). On the contrary, a decrease in the Raman ratio is obtained.

It was also observed that the absorbance increases again after 60 min, indicating an increase in the number of graphene layers. However, considering the evolution of the  $I_D/I_{2D}$  ratio, obtained by Raman spectroscopy (cf. Table 3), this new increase in the absorbance is accompanied by an increase in the  $I_D/I_{2D}$  ratio, indicating that we no longer have a simple separation of the layers, but rather a rupture of the C-C bonds. A treatment time of 5 min appears to be optimal.

**Table 3.** Evolution of Raman ratio after several ultrasonic time.

| Ultrasonic time (min) | $I_D/I_{2D}$ |
|-----------------------|--------------|
| 0                     | 0.55         |
| 5                     | 0.40         |
| 10                    | 0.39         |
| 30                    | 0.45         |
| 60                    | 0.46         |
| 90                    | 0.93         |

After this optimized HN treatment, CuO (Cu after Ar/5%H<sub>2</sub> treatment) nanoparticles were grown of the surface of the Gr materials treated [29]. Transmission electron microscopy (TEM) analysis shows that for the optimized growth and reduction heat treatment in a Ar/5% H<sub>2</sub> atmosphere, Cu particles with a mean diameter of  $16.8 \pm 7.1 \text{ nm}$  are grown of the Gr surfaces (cf. Figure 3).

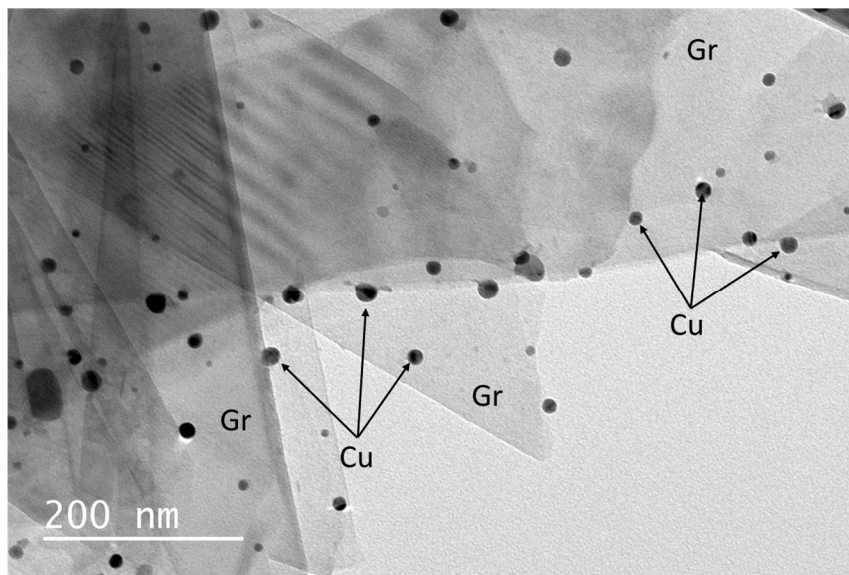


**Figure 3.** TEM micrograph of the Cu nanoparticles (black dots on the Gr surfaces) grown on the surface of treated HN Gr surfaces.

To verify the presence of a strong chemical bond between the copper nanoparticles and the surface of the reinforcement, an adhesion test was performed. The graphene solution was placed under an ultrasonic probe for 10 sec. As shown in Figure 4c, the copper nanoparticles (white dots on

the Gr surfaces) are still present on the surface of the reinforcement, although the particle density is slightly lower than the initial one (cf. Figure 4a). Another reinforcement was tested without a surface contamination removal pre-treatment (cf. Figure 4b). The copper nanoparticles were removed by the ultrasonic treatment due to the formation of bonds with the contamination present on the surface of the graphene, weakly bound to the reinforcement. Therefore, it is essential to eliminate this surface contamination.

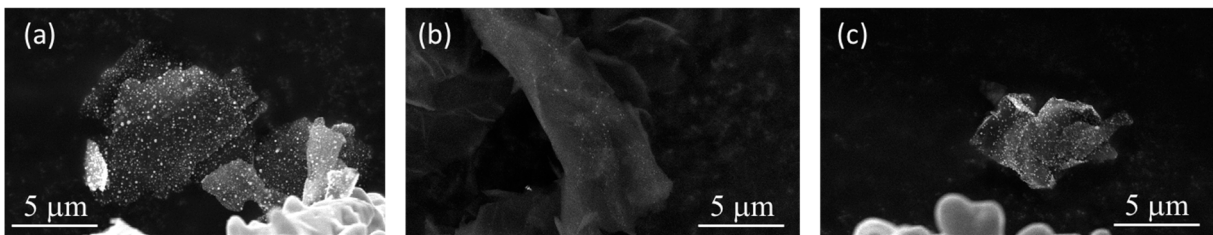


**Figure 4.** SEM micrograph of an (a.) graphene sheet with Cu(O) nanoparticles without HN pre-treatment, (b.) graphene sheet with Cu(O) nanoparticles without HN pre-treatment and after 10 sec of ultrasonic treatment, (c.) graphene sheet with Cu(O) nanoparticles with HN pre-treatment and after 10s of ultrasonic treatment.

### 3.3. Characterization of dense material

#### 3.3.1. Hardness

The material hardness was measured to highlight the impact of the reinforcement (cf. Table 4). As a reminder, an ultrasonic finger device and a germination method were used to individualize the graphene sheets to the maximum extent and optimize the electrical and mechanical properties of the material. Initially, it was observed that the simple introduction of the reinforcement does not induce a significant increase in the hardness of the different copper and copper alloys studied, due to the low amount of reinforcement present (0.06%Vol.). Secondly, it is noticed that carrying out an ultrasonic treatment induces a significant increase in material hardness, i.e., with an increase of about 12 HV for Cu-D/Gr. This result remains consistent because the reinforcements are a resistance to material deformation and the movement of dislocations. Therefore, the more particles present (induced by separating the sheets using ultrasonic treatment), the more the material hardness would increase. The evolution of material hardness is thus a relevant indicator to attest to the homogeneous distribution of reinforcement in the material, thereby optimizing the mechanical properties of the composite materials.

**Table 4.** Evolution of the hardness of different composite materials.

| Materials       | Hardness with/without ultrasonic treatment of the Gr (HV $\pm 1.2$ ) |         |
|-----------------|--|---------|
|                 | With   | Without |
| <b>Cu-D</b>     | 55.8   |         |
| <b>Cu-D/Gr</b>  | 55.3   | 67.6    |
| <b>Cu-P</b>     | 61.1   |         |
| <b>Cu-P/Gr</b>  | 61.5   | 72.4    |
| <b>Brass</b>    | 120.2  |         |
| <b>Brass/Gr</b> | 121.0  | 134.1   |

### 3.3.2. Electrical resistivity

The electrical resistivity measurements were carried out on our materials. The results are shown in Figure 5. Concerning the Cu-D/Gr composite, it can be observed that the decrease in electrical resistivity is only 1.4% compared to Cu-D without reinforcement. The introduction of Gr therefore has a relatively small impact on the electrical resistivity. Regarding Cu-P, which has higher electrical resistivity than Cu-D, the decrease in electrical resistivity (for the Cu-P/Gr composite) is more significant, with a gain of 2.7%. The reason for this greater decrease could be due to a more favourable alignment of the Gr layers in a plane perpendicular to the pressing direction. However, measurements carried out by polarized Raman spectroscopy (not presented in this study) disagree with this hypothesis.

To validate this hypothesis, a final series of materials were produced using brass (copper alloy with 20 wt.% of zinc) as the matrix, because brass has a higher electrical resistivity of  $6.8 \mu\Omega\text{.cm}$  than that of copper ( $1.75 \mu\Omega\text{.cm}$ ). The results of the electrical resistivity measurement show that the incorporation of graphene reduces the electrical resistivity for approximately 10%.

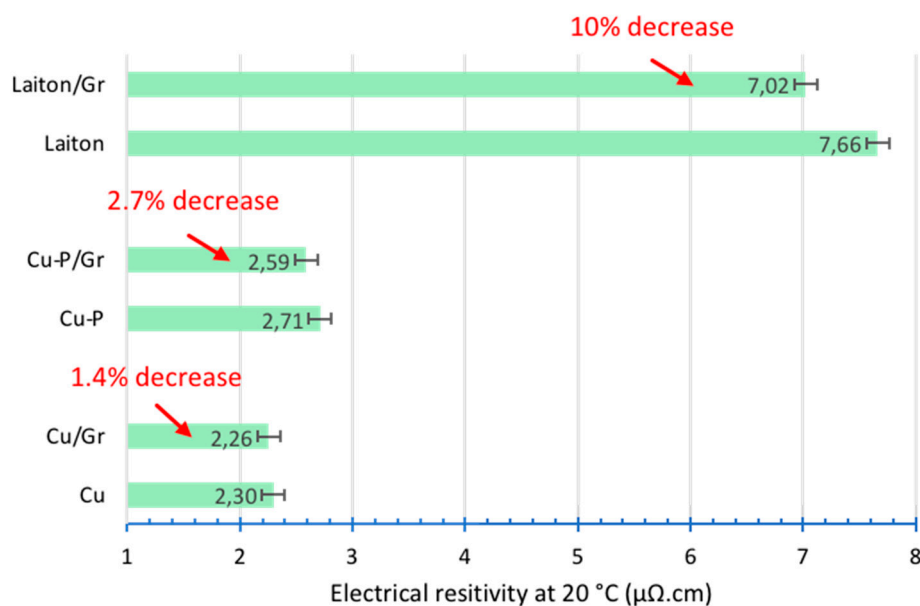


**Figure 5.** Electrical resistivity measurement at 20 °C for various single and composite copper matrix materials.

## 4. Conclusions

In this study, a new method for developing Cu/Gr composites was developed, with significant focus on creating a high-performing interface through the germination growth of the CuO nanoparticles. Hardness measurements showed the importance of separating Gr layers to obtain a homogeneous distribution, resulting in increased material hardness. Results from electrical resistivity measurements indicated that using a matrix with higher resistivity than Cu leads to a greater positive composite effect. This validates our hypothesis and highlights that the intrinsic properties of Gr used are not sufficient for achieving a significant positive composite effect on Cu-D. This finding suggests the possibility of incorporating graphene into lower quality copper or copper alloys to increase their electrical conductivity and reduce the amount of copper used, especially considering the shortage of copper resources expected to occur within the next fifty years. Furthermore, incorporating graphene reinforcement into materials with higher electrical resistivity, such as ferrous or Al alloys, may be feasible, although optimizing the R-M interfaces using an appropriate metallic salt will be necessary.

**Author Contributions:** The work was completed through contributions of all authors. All authors have given approval to the final version of the manuscript. The individual contributions are: supervision and conceptualization: Jean-François SILVAIN, Nathalie CAILLAULT, Florence DELANGE; manuscript writing: Jean-François SILVAIN, Yongfeng LU, Antoine BIDENT; material elaboration and characterizations: Antoine BIDENT.

**Data and materials availability:** All data needed to support the conclusions in the paper and the datasets generated during the current study are available from the corresponding author on reasonable requests.

**Acknowledgments:** This study was supported by Schneider Electric SAS.

**Competing Interests:** The authors declare no competing financial interest.

## References

1. Copper Alliance, <https://copperalliance.fr/le-cuivre/le-cuivre-dans-lhistoire/>
2. IEA, <https://www.iea.org/reports/electricity-information-overview/electricity-production>
3. Boursorama, <https://www.boursorama.com/bourse/matieres-premieres/cours/7xCAUSD/>
4. K. S. Novoselov, A.K. Geim, S.V. Morozov, D. Jiang, Y. Zhang, S.V. Dubonos, I.V. Gogorieva, A.A. Firsov, Electric Field Effect in Atomically Thin Carbon Films, *Science* 306(5696) (2004) 666-9. DOI: 10.1126/science.1102896
5. A. H. C. Neto, F. Guinea, N.M.R. Peres, K.S. Novoselov, A.K. Geim, The electronic properties of graphene, *Rev. Mod. Phys.* 81 (2009) 109. <https://doi.org/10.1103/RevModPhys.81.109>
6. P. R. Wallace, The Band Theory of Graphite, *Phys. Rev.* 71 (1947) 622. <https://doi.org/10.1103/PhysRev.71.622>
7. K. I. Bolotin, K.J. Sikes, Z. Jiang, M. Klima, G. Fudenberg, J. Hone, P. Kim, H.L. Sormer, Ultrahigh electron mobility in suspended graphene, *Solid State Communications* 146(9) (2008) 351-355. <https://doi.org/10.1016/j.ssc.2008.02.024>
8. P.A. Kohyakov, G. Giovannetti, P.C. Rusu, G. Brocks, J. van den Brink, P.J. Kelly, First-Principle study of the interaction and charge transfer between graphene and metals, *Physical review B* 79 (2009) 195425. <https://doi.org/10.1103/PhysRevB.79.195425>
9. C. Lee, X. Wei, J.W. Kysar, J. Hone, Measurement of the Elastic Properties and Intrinsic Strength of Monolayer Graphene, *Science* 321(5887) (2008) 385-8. DOI: 10.1126/science.1157996
10. P.N. Nirmalraj, T. Lutz, S. Kumar, G.S. Duesberg, J.J. Boland, Nanoscale Mapping of Electrical Resistivity and Connectivity in Graphene Strips and Networks, *Nano Lett.* 11(1) (2011) 16-22. DOI: 10.1021/nl101469d
11. W. Li, Y. Liu, G. Wu, Preparation of graphite flakes/Al with preferred orientation and high thermal conductivity by squeeze casting, *Carbon* 95 (2015) 545-551. <https://doi.org/10.1016/j.carbon.2015.08.063>
12. C. Azina, Diamond-based multimaterials for thermal management applications, University of Bordeaux, PhD thesis (2017)
13. G. Giovannetti, P. A. Khomyakov, G. Brocks, V. M. Karpan, J. van der Brink, P.J. Kelly, Doping graphene with metal contacts, *Phys. Rev. Lett.* 101 (2008) 026803. <https://doi.org/10.1103/PhysRevLett.101.026803>
14. M. Li, H. Che, X. Liu, S. Liang, H. Xie, Highly enhanced mechanical properties in Cu matrix composites reinforced with graphene decorated metallic nanoparticles, *J. Mater. Sci.* 49(10) (2014). DOI:10.1007/s10853-014-8082-x
15. H. Luo, Y. Sui, J. Qi, Q. Meng, F. Wei, Y. He, Copper matrix composites enhanced by silver/reduced graphene oxide hybrids, *Materials Letters* 186 (2017) 354-357. 10.1016/j.matlet.2017.03.084
16. K. S. Kappagantula, J.A. Smith, A. Nittala, F. Kraft, Macro Copper-Graphene Composites with Enhanced Electrical Conductivity, *Journal of Alloys and Compounds* 894 (2001) 162477. DOI:10.1016/j.jallcom.2021.162477
17. M. Cao, D.B. Xiong, L. Yang, S. Li, Y. Xie, Q. Guo, Z. Li, H. Adams, J. Gu, T. Fan, X. Zhang, D. Zhang, Ultrahigh Electrical Conductivity of Graphene Embedded in Metals, *Adv. Funct. Mater.* 29(17) (2019) 1806792. <https://doi.org/10.1002/adfm.201806792>
18. C. Ayyappadas, A. Muthuchamy, A. Raja Annamalai, D.K. Agrawal, An investigation on the effect of sintering mode on various properties of copper-graphene metal matrix composite, *Advanced Powder Technology* 28(7) (2017) 1760-1768. doi: 10.1016/j.apt.2017.04.013
19. L.L. Dong, W. Chen, C. Zheng, N. Deng, Microstructure and properties characterization of tungsten-copper composite materials doped with graphene, *Journal of Alloys and Compounds* 695 (2016). DOI:10.1016/j.jallcom.2016.10.310
20. M. Fluke, R. Kleinrahm, et W. Wagner, Measurement and correlation of the (p, ρ, T) relation of nitrogen II. Saturated-liquid and saturated-vapour densities and vapour pressures along the entire coexistence curve, *The Journal of Chemical Thermodynamics* 34(12) (2002) 2017-2039. DOI:10.1016/S0021-9614(02)00266-5
21. B. Alemour, M. H. Yaacob, M.R. Hassan, Review of Electrical Properties of Graphene Conductive Composites, *International Journal of nanoelectronics and Materials* 11(4) (2018) 371-398.

22. A. Bident, Elaboration de matériaux composites cuivre/graphène à propriétés physiques améliorées par métallurgie des poudres, PhD thesis (December 2022) University of Bordeaux, France
23. A.H. Neto, F. Guinea, N.M.R. Peres, K.S. Novoselov, A.K. Geim, The electronic properties of graphene, *Reviews of Modern Physics* 81 (2009) 109-155, DOI: 10.1103/RevModPhys.81.109

**Disclaimer/Publisher's Note:** The statements, opinions and data contained in all publications are solely those of the individual author(s) and contributor(s) and not of MDPI and/or the editor(s). MDPI and/or the editor(s) disclaim responsibility for any injury to people or property resulting from any ideas, methods, instructions or products referred to in the content.